Monochromatic Mean Wavelength Calculation and Refractivity of Air Inference by Michelson Interferometer Analysis

Ryan White
44990392

12th of June 2020

Abstract

Using a typical michelson interferometer setup, the average wavelength of monochromatic light (emitted from a sodium lamp source) was calculated by linear regression techniques after experimentation in dark-room laboratory conditions. By altering the setup to include a variable pressure chamber, the refractivity of air was inferred (also by linear regression across multiple averaged data points) and compared to quoted values from other studies. Practical applications of the data obtained were implied, with changes in the context of future studies suggested based on shortfalls in the measured data range.

1 Introduction

The field of optics is integral to everyday life, with a broad range of applications that are considered essential for modern civilisation relying on the fundamental physics described by optics. The Michelson Interferometer is perfect practical visualisation of various underlying theories of optics, with vast applications to modern science such as the LIGO direct observation of gravitational waves and fibre optic internet cables. The experiment is performed via the splitting of a beam of light, which is then ejected to and reflected from two different mirrors and consequently interferes with the other half of the beam at the wavesplitter. Interference effects are observed as a result of this superposition, and various fundamental variables of electromagnetic waves may be calculated and inferred from observation of the resultant interference patterns. This experiment aims to investigate the effect of varying the path length difference of a split beam of light on the wavelength and amplitude of light, as well as the varying of chamber pressure of a refracting gas to determine the refractivity of air.

2 Theory

According to figure 1, after a beam of light is ejected from a central beamsplitter in the direction of a mirror M_2, it will travel some extra distance (denoted the path length difference, or $\Delta r = 2d$) compared to an equivalent wave of light (ejected in a perpendicular direction) that reflects off of mirror M_1, where both waves were initially emitted from the sodium lamp source. After these two beams meet at the beamsplitter and interfere, constructive or destructive interference ensues according to

$$2d\cos\theta = m\lambda \tag{1}$$

where d is the distance M_2 was translated, θ is the angle of the waves relative to each other and λ is the wavelength of the light emitted from the source. Equation (1) describes the intereference impact on the spectrum of constructive to destructive via the variable m fringe order, where $m \in \mathbb{Z}^+$ corresponds to destructive interference, and $m \in \frac{1}{2}\mathbb{Z}^+$ shows constructive interference.
In order to calculate the effective average wavelength across the experiment iterations, the equation

$$2d = m_0\lambda$$

where m_0 is the order of the central fringe, may be rearranged to give

$$\lambda = \frac{2d}{m} = \frac{\Delta r}{m} \tag{2}$$

Using similar practices, the refractivity of air may also be calculated via the use of a pressure chamber with glass interfaces separating the gas from the atmospheric environment. As light passes slower than c through a medium, the thickness, or rather refractive index, of the medium dictates the speed at which light transverses. The velocity change is analogous to a change in distance (in a vacuum), with the relationship described by (via PHYS2055 Laboratory Notes)

$$\Delta r = (n-1)l \tag{3}$$

where n is the refractive index of the gas, and l is the length of the pressure chamber. Here, the term $n-1$ is called the refractivity of the gas, symbolising the difference in refractive index of the gas from that of a vacuum (which has $n = 1$). Of course, the refractivity of the gas may easily be solved by

$$n - 1 = \frac{\Delta r}{l} \tag{4}$$

where Δr may be inferred via linear regression of experimental data.

Unless otherwise stated or derived, the above equations were reference from Griffiths *Introduction to Electrodynamics*.

3 Experiment

3.1 Experimental Setup

The experimental apparatus used to test the interference effects were arranged according to figure 1.

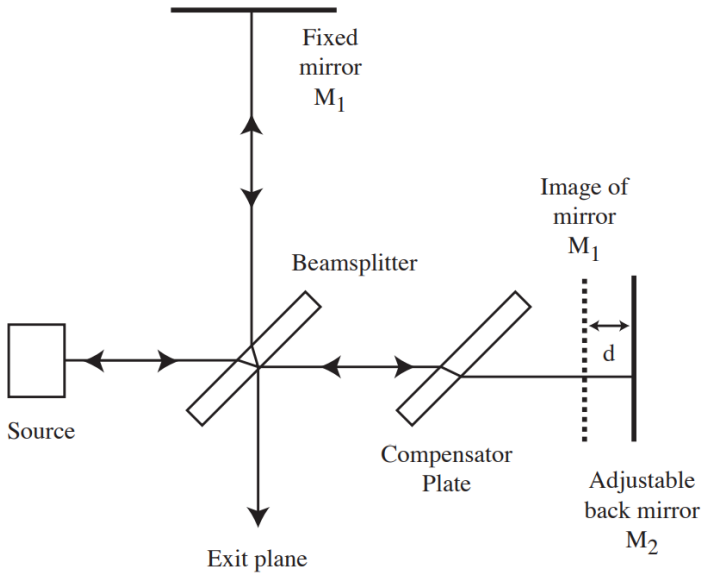

Figure 1: Schematic Diagram of Michelson Interferometer - Part 1

Source: PHYS2055 Michelson Interferometer Notes

3.1.1 Part 1 - Measurement of Mean Wavelength/Wavelength Separation

Firstly, the lights in the laboratory were turned off, with only dim light illuminating the workspace from a computer monitor situated to the left of the source lamp seen in figure 1. Monochromatic light was emitted from the sodium lamp source at a wavelength of 589nm. The fixed mirror M_1 was neither tilted nor translated in any direction, while the adjustable mirror M_2 was able to be translated along the x-axis of figure 1 by some distance d via the turning of a dial not pictured. Each division on the dial corresponded to a translation of the mirror of 250nm in the positive x-direction (i.e. to the right direction in the figure). A webcam was placed at the position of the exit plane in the figure, which was connected to a computer with Logitech Webcam Software, with the settings shown in Appendix 7.3. On the software, two parallel lines (roughly a distance apart of the width of a visible fringe) were superimposed onto the screen in order to accurately count the fringe pattern cycles.

3.1.2 Part 2 - Measuring the Refractivity of Air

The experimental setup was largely similar to that of Part 1, with only a few key differences. Firstly, an air chamber, measuring approximately 87±1mm long with glass screen thickness of approximately 2±0.5mm, was placed in front of the fixed mirror M_1. The air chamber was connected to a manual air pump, complete with an analogue pressure gauge.

3.2 Method

Beginning at the 0 division on the dial mentioned in section 3.1.1, the dial was rotated anticlockwise by 5 divisions while simultaneously counting the fringes passing through the parallel lines on the webcam software. The number of fringes was recorded, and the dial was rotated clockwise slowly until it was returned to the 0 point. This process was repeated several more times, with the divisions that the dial was rotated being increased by 5 ticks each iteration, up to a final iteration of 60 ticks.

For the second part of the experiment, the equipment was setup according to the description in section 3.1.2. Using the manual air pump, the pressure inside the air chamber was increased to 100mmHg, and was held at this pressure until ready to record. The pressure was slowly released, approaching a final pressure of 78mmHg, while simultaneously counting the fringes passing through the parallel lines superimposed onto the webcam software. The cycle count was recorded, and the process repeated in increasing initial pressure intervals of 20mmHg up to a last iteration initial pressure of 220mmHg.

3.3 Uncertainties

As with any experiment performed with human intervention, there were a host of uncertainty sources that were addressed. Firstly, there was uncertainty in the value of the dial division which was estimated to be about ± 0.2 divisions (chosen to be the smallest significant value observable on the dial). This uncertainty corresponds to approximately ± 50nm of translation distance of the mirror M_2. As the interference fringes were counted discretely, there was assumed to be negligible uncertainty in the count. As for the second part of the experiment, the pressure gauge was deemed to have an uncertainty of the smallest visible increment distance, ± 2mmHg.
All uncertainty propagation was carried out according to Appendix 1.

4 Results

The raw data, including aforementioned uncertainties, are available in tables 1 and 2.

Ticks (± 0.2)	Distance (nm) (± 50nm)	Cycle Count
5	1250	4
10	2500	9
15	3750	13
20	5000	17
25	6250	14
30	7500	18
35	8750	23
40	10000	27
45	11250	32
50	12500	45
55	13750	41
60	15000	46

Table 1: Cycle Count of Interference Fringes Against Mirror Translation Distance

As can be seen, the cycle count increase is largely linear with infrequent 'jumps' to local extrema. This is clearer in figure 2 below

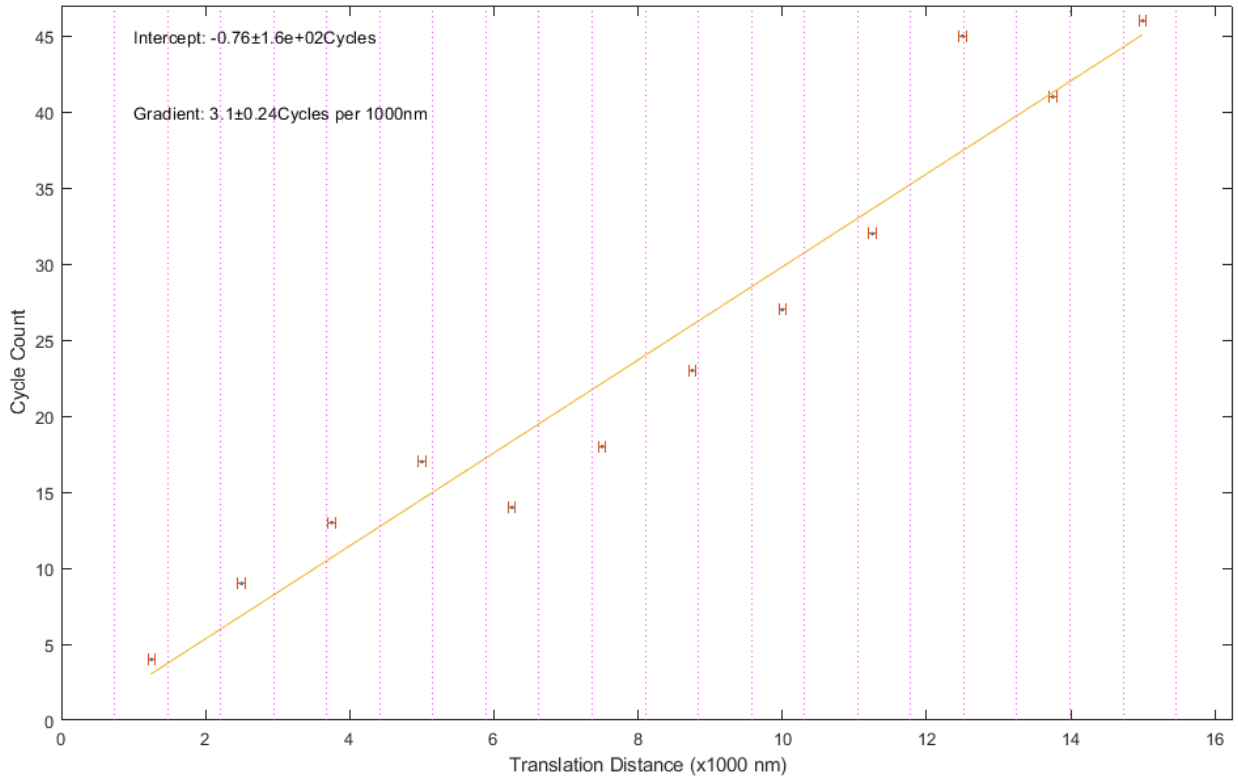

Figure 2: Cycle Count vs Mirror Translation Distance

The above figure shows the locally linear relationship between increasing translation distance and interference fringe cycle count. To aid in the later investigation, magenta vertical lines were added to show the multiples of the source light wavelength. Particularly at $d = 12500$nm (or the 17th multiple of the sodium lamp wavelength), there was a large increase in the recorded cycle count likely due to the total constructive interference.
To measure the refractivity of air, the experimental setup was changed in accordance with section 3.1.2. The data recorded across the method is available in table 2

P_i (mmHg) (±2mmHg)	ΔP (mmHg) (±3mmHg)	Cycle Count
100	22	2
120	42	5
140	62	7
160	82	9
180	102	11
200	122	17
220	142	22

Table 2: Cycle Count Against ΔP to Reach 78 mmHg

As with the data from the first part of the experiment, the cycle count increase seemed to follow a roughly

linear trend until the final few iterations. This statement is further supported by figure 3

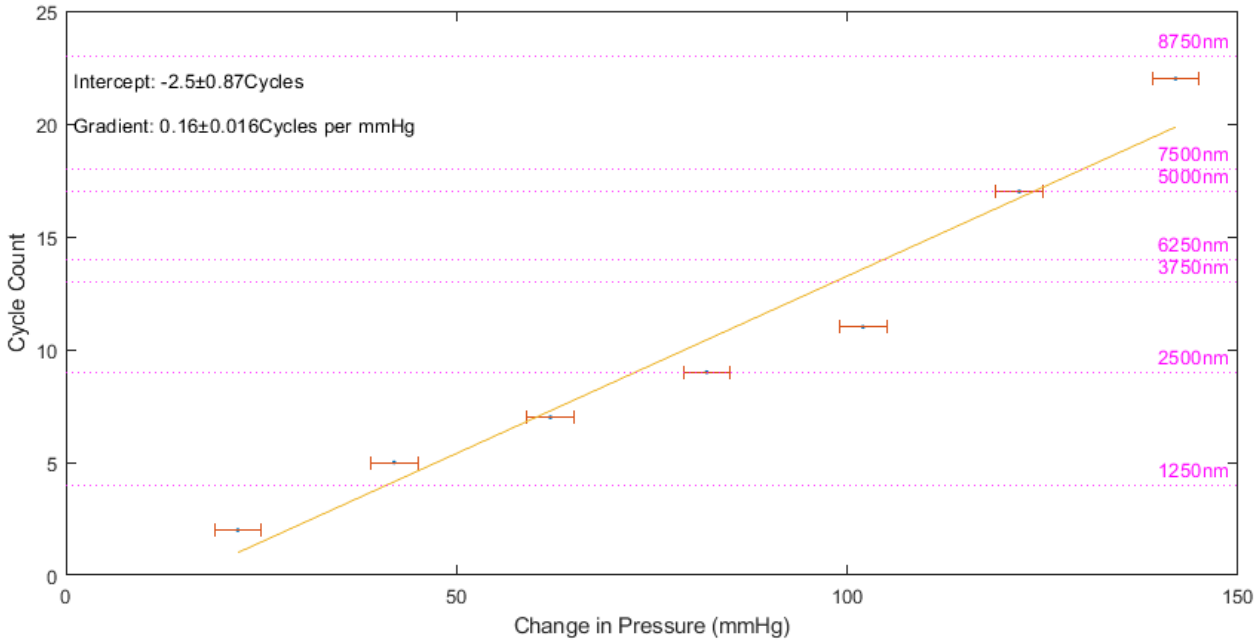

Figure 3: Cycle Count vs Mirror Translation Distance

The above figure shows the aforementioned linear trend in the initial iterations of the procedure, and has superimposed "distance" comparisons corresponding to the equivalent cycle count value taken from table 1.

5 Discussion

The average wavelength of the light observed through the webcam was easily be inferred from figure 2. As calculated via linear regression, the average trendline was characterised by a gradient of 3.1 ± 0.24 Cycles per 1000nm translation distance of the mirror M_2. This corresponded to a change of 3.1 ± 0.24 Cycles per 2000nm path length difference change. By rearranging the variables, this equated to an approximate wavelength of 650±60nm (uncertainty propagated in Appendix 7.2.2), which was clearly within reasonable bounds of the quoted wavelength of a sodium lamp (589nm) especially when considering human error in the experiment.

The refractivity of air was easily be calculated via equation (4), stated in the Theory section above. The path length difference, however, was not directly measured in the experiment. Instead, the linear regression code (created in the linear regression exercise) gave all the appropriate tools to infer the equivalent path length difference. Firstly, the atmospheric pressure expressed in terms of millimeters of mercury is about 1atm = 760mmHg. With this, the gradient calculated and shown in figure 3 was used to extrapolate a cycle count of approx 110 ± 11 cycles as the pressure decreased from atmospheric pressure to 78mmHg ($\Delta P = (760 - 78) \times 0.16 = 110$ Cycles). This was then expressed in terms of an effective multiple of 1000nm by rearrangement of the gradient given in figure 2 to give a multiple of approximately 35 ± 4.5 times 1000nm, or rather a path length difference of approximately 35000 ± 4500nm. From here, equation (4) was used

together with the quoted length of the pressure chamber

$$\begin{aligned} n - 1 &= \frac{\Delta r}{l} \\ &= \frac{35000 \times 10^{-9}\text{m}}{87 \times 10^{-3}\text{m}} \\ &= 4.023 \times 10^{-4} \\ &\approx 4 \times 10^{-4} \end{aligned}$$

With uncertainty propagation, this refractivity value for air was given at approximately $(4 \pm 0.5) \times 10^{-4}$. By [2], the refractivity of dry air at atmospheric pressure and 15°C is approximately 3×10^{-4}. Considering that the laboratory conditions of this experiment were at higher temperatures and with non-zero humidity values (which would significantly increase the refractivity), the calculated value that is 33% higher was deemed reasonable.

6 Conclusions

Through the use of the michelson interferometer in dark-room laboratory conditions, the mean wavelength of superpositioned monochromatic light was determined across several translation values for a varying-position reflective mirror. An average wavelength of approximately 650 ± 60nm was calculated, and considering that the source wavelength was quoted as approximately 589nm, the calculation was deemed reasonably accurate. In the second part of the experiment, the refractivity of air was determined by the analysis of a varying-delta pressure pressure chamber, where an effective path length difference was inferred and used to calculate the resultant refractivity. A value of $(4 \pm 0.5) \times 10^{-4}$ was calculated, and compared with a quoted value of 3×10^{-4} for dry air at atmospheric pressure and 15°C.
The experimental data recorded was largely very useful in analysis, however there are always ways that a methodology can be improved. One such suggestion is the measurement of the cycle count particularly around some Δr that is a multiple (or half multiple) of the source wavelength in order to further investigate the effects of constructive and destructive interference.

7 Appendices

7.1 Uncertainty Calculations/Propagations Formulae

All uncertainties were propagated according to the rules shown in Table 4

Relationship	Uncertainty obtained from
General expression	
$p = f(x,y,z,\ldots)$	$(\Delta p)^2 = \left(\frac{\partial f}{\partial x}\Delta x\right)^2 + \left(\frac{\partial f}{\partial y}\Delta y\right)^2 + \left(\frac{\partial f}{\partial z}\Delta z\right)^2 + \ldots$
Specific cases	
$p = x + y$	$\Delta p = \sqrt{(\Delta x)^2 + (\Delta y)^2}$
$p = x - y$	$\Delta p = \sqrt{(\Delta x)^2 + (\Delta y)^2}$
$p = x\,y$	$\frac{\Delta p}{\lvert p\rvert} = \sqrt{\left(\frac{\Delta x}{x}\right)^2 + \left(\frac{\Delta y}{y}\right)^2}$
$p = \frac{x}{y}$	$\frac{\Delta p}{\lvert p\rvert} = \sqrt{\left(\frac{\Delta x}{x}\right)^2 + \left(\frac{\Delta y}{y}\right)^2}$
$p = Bx$	$\Delta p = B\,\Delta x$
$p = Ax^n$	$\frac{\Delta p}{p} = n\frac{\Delta x}{x}$
$p = \log x$	$\Delta p = \frac{1}{2.3x}\Delta x$
$p = \sin\theta$	$\Delta p = \lvert\cos\theta\rvert\,\Delta\theta$

Figure 4: Uncertainty Propagation Formulae

Source: PHYS2055 Linear Regression Document

In uncertainty propagations, the uncertainty was denoted by δ instead of Δ to avoid confusion in 'change in' variables.

7.2 Example Uncertainty Propagations

7.2.1 Uncertainty Propagation in Table 2

$$\begin{aligned} \delta p &= \sqrt{(\delta x)^2 + (\delta y)^2} \\ \Rightarrow \delta\Delta P &= \sqrt{(\delta P_i)^2 + (\delta P_f)^2} \\ &= \sqrt{2^2 + 2^2} \\ &= 2.83 \approx 3\text{mmHg} \end{aligned}$$

7.2.2 Uncertainty Propagation for Mean Wavelength Calculation

$$\begin{aligned}
\frac{\delta p}{|p|} &= \sqrt{\left(\frac{\delta x}{x}\right)^2 + \left(\frac{\delta y}{y}\right)^2} \\
\Rightarrow \delta\lambda &= \lambda\sqrt{\left(\frac{\delta \text{Cycles}}{\text{Cycles}}\right)^2 + \left(\frac{\delta d}{d}\right)^2} \\
&= 650\sqrt{\left(\frac{0.24}{3.1}\right)^2 + \left(\frac{100}{2000}\right)^2} \\
&= 59.9 \approx 60\text{nm}
\end{aligned}$$

7.3 Settings of Logitech Webcam Software

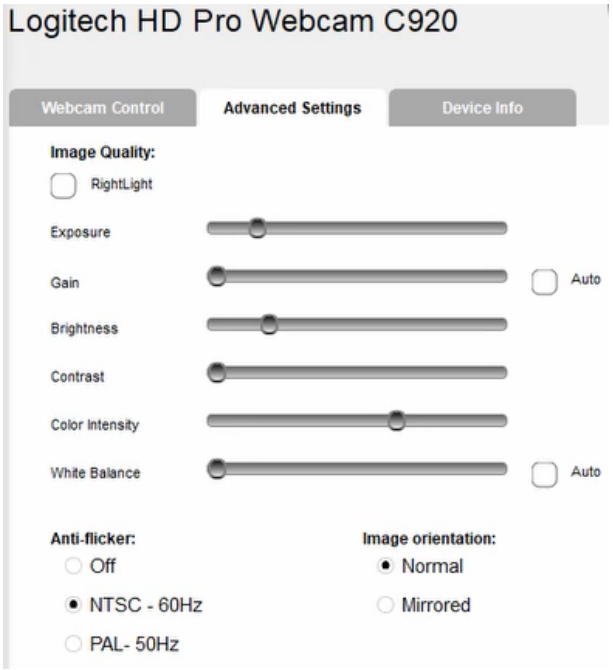

Figure 5: Logitech Webcam Settings Used

References

[1] Griffiths, D. 2017. *Introduction to Electrodynamics*. 4th ed. United Kingdom: Cambridge University Press.

[2] Young, A. 2019. *Refractivity of Air*. Available at: https://aty.sdsu.edu/explain/atmos_refr/air_refr.html [Accessed 12th of June, 2019]